DESIGN AND CONTROL OF A PERMANENT MAGNET SYNCHRONOUS MOTOR DRIVE FOR A HYBRID ELECTRIC VEHICLE

S. Van Haute*, St. Henneberger*, K. Hameyer*, R. Belmans*
J. De Temmerman**, J. De Clercq**

* Katholieke Universiteit Leuven; Belgium
** Inverto N.V.; Belgium

Abstract The design and control of a 45 kW 6-pole permanent magnet synchronous motor (PMSM) with surface-inset magnets for a hybrid electric vehicle is described. The advanced field weakening strategy takes advantage of the additional reluctance torque. The influence of the saturation effects on the motor torque is considered by computing the inductances L_d and L_q are for each operational point. The accurate prediction of the motor performance is essential for the optimal control of the drive over a wide range of operation. The drive control is implemented on a DSP based, MATLAB®/SIMULINK® programmable hardware system.

INTRODUCTION

Hybrid electric vehicles have the advantage to operate with zero emission in the inner city while not being limited in the range for intercity distances. Furthermore, the possibility of regenerating the braking energy is offered.

The main parts of the drive equipment are the energy sources, in this study a Diesel generator connected in parallel to a rechargeable NiCd traction battery, the traction motor with converter and controller, and the main controller unit. The drive module is connected to a main controller collecting the status information: acceleration, deceleration, regenerating the braking energy, etc. (Fig. 1). The desired torque T_d given by the driver of the vehicle is processed by the main controller.

The heart of the drive consists of the permanent magnet excited synchronous machine. [PMSM]. The possibilities of such type of motors for road electric traction was already investigated in the early eighties by Sneyers et al [a,b]. An electric vehicle motor design requires high efficiency, extended field weakening range, high power/weight ratio and high reliability. Water cooling, high energy density permanent magnets and special control strategies (], are applied in order to fulfil these requirements.

One of the main design goals for the studied drive system is the continuous operation of the PMSM at high efficiency. Therefore, a rotor geometry with $X_q > X_d$ is chosen to benefit from an additional reluctance torque (Fig.1) (Jahns et al [d],]). The rotor design causes a disadvantage for the motor control: the machine parameters are dependent on the operating point due to saturation effects. As a real time control strategy is essential to assure the continuous operation at highest efficiency, those dependencies have to be known in advance. The control algorithm then directly operates on the pre-calculated set of performance characteristics in form of tables or polynomial functions.

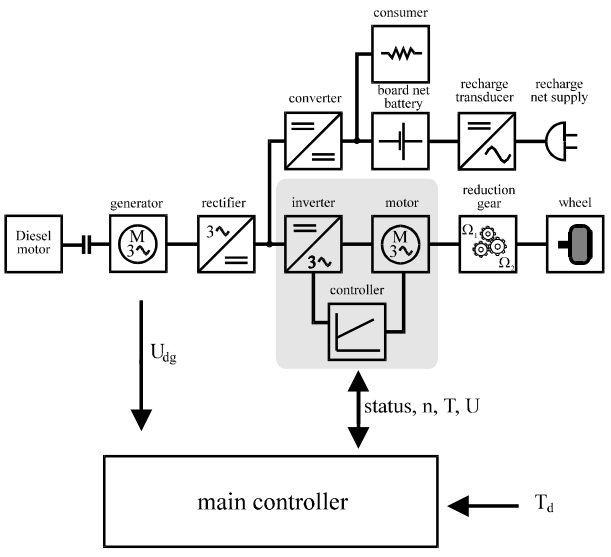

Figure 1 Topology of the hybrid drive concept.

The design procedure takes advantage of analytical calculations as well as static Finite Element Analysis (Chang et al [2], Slemon et al [3]) and thermal computations.

Apart from the feedforward torque control, several algorithms for flux-weakening have been published recently, including current and voltage limitation and compensation of cogging torque [6,i,j]. A general flux-weakening algorithm is adapted. to the designed motor, simulated and implemented on a DSP based hardware system using a MATLAB®/SIMULINK® programmable control environment. The optimal negative direct axis current is determined for operating points both in constant torque region as in constant power region.

The experimental setup further includes a modified standard inverter for induction motors and a reduced scale prototype motor.

MOTOR DESIGN

PMSMs are usually classified into surface mounted permanent magnet motors (SPMSM) and interior or buried permanent magnet motors (IPMSM) [d,1]. The first can have sinusoidal back emf, but have limited field weakening capabilities, due to relatively small inductance values. The latter has higher inductances and thus an extended constant power operation range. Moreover, because direct and quadrature inductance are not equal, a reluctance torque contributes to the total motor torque. However, the back emf is no longer sinusoidal.

A motor design as shown in figure 2 can combine some advantages of the above mentioned motor types. This motor is referred to as a *surface-inset* PMSM (Sebastian and Slemon [e]). As in the IPMSM, due to magnetically asymmetrical rotor design, the total torque has an electromagnetic component and a reluctance component.

In order to achieve a high efficiency of the PMSM the losses have to be kept low being contrary to a high power/weight ratio. Therefore, the optimal choice of the desired low weight and acceptable iron losses has to be made. In the same way, the contributing losses can be reduced by using more winding copper, yielding in increasing costs and additional weight. The thickness of the iron yoke is reduced by applying a high number of poles. However, the number of poles is limited by the frequency of the inverter, and furthermore, a wide range of field weakening can only be achieved by a relatively small

number of poles (Hadji Minaglou [5]). Iron losses are further decreased by choosing thin low-loss lamination in the stack of the stator. The power/weight ratio is further improved by applying an indirect water cooling system.

A high L_d value extends the field weakening range, however increasing L_d by decreasing the thickness of the permanent magnets has limits. It enables their demagnetisation and reduces the reluctance torque by decreasing the ratio L_q/L_d.

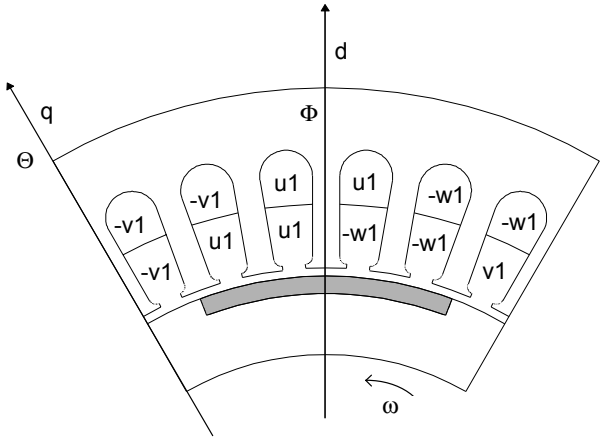

Figure 2. Cross-sectional view of a 6-pole surface-inset PMSM.

Another design aspect is the choice of the permanent magnet material. A high remanent flux density is needed, while a high coercivity is less important as overloads do not occur. NdFeB permanent magnets offer a high energy density as well as a high remanence flux density. Furthermore, the operating high temperatures are no longer a drawback as the new generation of NdFeB magnets (VACODYM 411) retains its magnetic properties up to high temperatures of 120º C.

Using surface mounted magnet pieces, glued onto the rotor, instead of one magnet piece for one pole, reduces eddy current losses and herewith the heating of the magnets.

The design procedure results in a motor design (Fig. 2) of which the dimensions are summarised in table 1, fulfilling the performances listed in table 2. The torque/speed characteristic, showing the field weakening range (Figure 3), is computed by calculating the operating points of the equivalent circuit of the machine. The equivalent circuit is calculated as function of the rotor torque angle δ as well as the terminal current, due to the fact that the inductances are dependent of the current components I_d and I_q. The mechanical torque is calculated as function of the supplied voltage and the stator current. Figure 4 shows the terminal voltage, the stator current and the efficiency as function of the speed.

Tab. 1 Dimensions of the PMSM

Stack OD	299 mm
Stack ID	208 mm
Rotor length	130 mm
Overall mass	60.4 kg
Number of poles	6

Tab. 2 Performances of the PMSM

power/weight ratio	0.8 W/kg
weakening range n_{max}/n_r	2.8
efficiency	96,2 %

PMSM WITH EXTENDED FIELD WEAKENING

The motor operates in an advanced field weakening mode by implementing a negative direct stator current in order to benefit from the reluctance torque. The motor can be operated in two modes. In the constant torque mode, the speed of the drive is increased by raising the stator frequency and voltage until rated speed is reached. To increase speed further, power and voltage have to be maintained constant while increasing the angle between stator current and field axis above 90º by additionally applying a negative direct stator current component (Fig. 3). The required current is minimized and the possibility of irreversibly demagnetizing the magnets is reduced. The significant saliency of the motor, realized by constructing a rotor with surface-inset magnets (Fig. 2), is generating a reluctance torque.

Direct and quadrature axis current components are calculated by Parks transformation and fed to the control algorithm (Figure 5). In d-q coordinates, the dynamic behaviour of a PMSM is described by the following set of equations.

$$u_d = R.i_d - \omega L_q.i_q + pL_d i_d \quad (3)$$

$$u_q = R.i_q + \omega L_d.i_d + pL_q i_q + \omega\phi_f \quad (4)$$

The torque equation is a function of the angle $\Psi = 90º-\delta$ and can be splitted into an electromagnetic component (1) and a reluctance component (2)

$$T_e(\Psi) = \frac{m \cdot p}{\omega_0} \cdot E \cdot I_q \,, \quad (1)$$

$$T_r(\Psi) = m \cdot p \cdot I_d \cdot I_q \cdot (L_q - L_d), \quad (2)$$

where $I_d = I \cdot \sin(\Psi)$, $I_q = I \cdot \cos(\Psi)$ with *m* - the number of phases, *p* - the number of poles, ω_0 - the synchronous angular speed and *E* - the fundamental e.m.f..

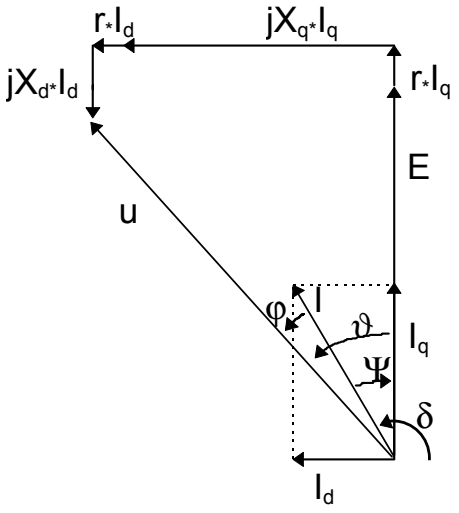

Figure 3. Phasor diagram of the PMSM in the advanced field weakening mode.

The motor is controlled by adjusting the load angle to obtain the maximum torque $T_{max} = T_e + T_r$ which is expressed as a function of the angle $\Psi = 90º-\delta$ by the equation

$$\Psi_{opt} = \arcsin\left(\frac{E}{4I_1\omega\left(L_q - L_d\right)} - \sqrt{\left(\frac{E}{4I_1\omega\left(L_q - L_d\right)} \right)^2 + \frac{1}{2}} \right). \qquad (3)$$

The load angle, being a measure for the ratio of the current in the direct axes versus the total current in the stator with $I_d = I \cdot \sin(\Psi)$ is described as a function of the speed for different values of the current in the stator:

$$\sin(\Psi) = \frac{\frac{u_{max}^2}{n^2} - e^2 - \left(x_{d0}^2 \cdot i^2\right)}{2 \cdot e \cdot x_{d0} \cdot i} \qquad (4)$$

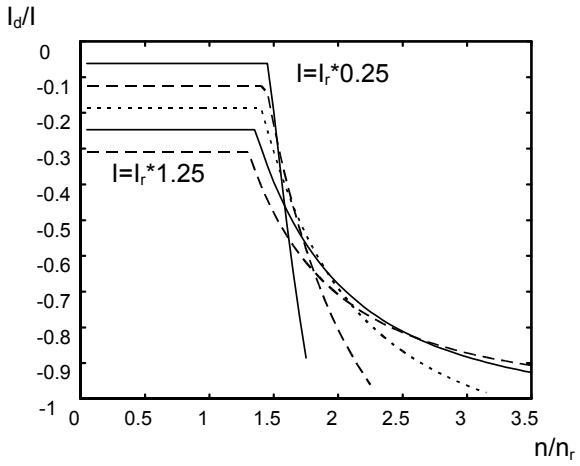

Figure 4. I_d/I for different arature currents as function of the speed .

NUMERICAL COMPUTATION

Due to saturation effects in the stator teeth and the rotor iron in the interpolar region, the inductances L_d and L_q are a function of the stator current and the load angle or, in other words of the current components I_d and I_q. [d].They have to be known for each possible state of operation in order to accurately control the machine as well as to simulate the dynamic behaviour of the machine. In the past, some attempts were done to correct the classical mathematical model by introducing cross-coupling terms [b],[c].

The application of the finite element analysis for the determination of the lumped parameter model and the performance of the PMSM have been discussed widely in the literature [5],Nipp [6]. As shown in [5], the FE analysis is suited for the calculation of the PMSM utilizing rotor geometry with $X_q > X_d$.

A high number of FE model evaluations is performed in order to have knowledge of the machine parameters in a variety of operating points. These data are used in off-line simulations, and can be used in simple, parameter dependent real-time control schemes.

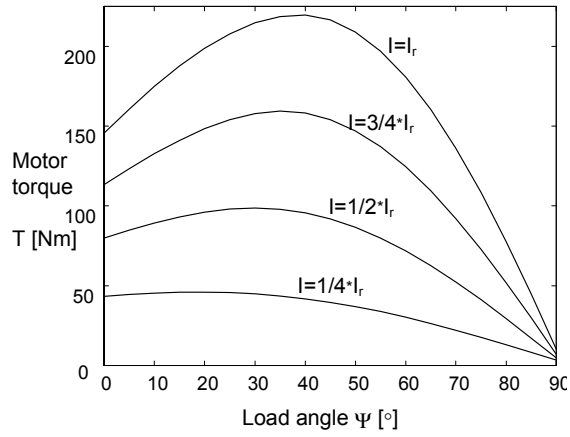

Figure 5. Numerical computed overall torque as function of the load angle at different stator currents.

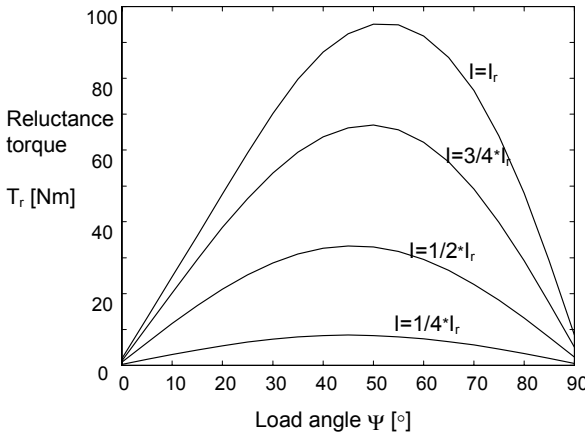

Figure 6. Numerical computed reluctance torque as function of the load angle at different stator currents.

The calculation of the inductances L_d and L_q as a function of the load angle δ_1 is straightforward, applying a flux linkage method. Formulation (4) Henneberger et al [4] provides the general tool to compute the inductance of a winding in two dimensions,

$$L = \frac{l_z}{i^2} \int_S A_z \cdot J \, dS \qquad (4)$$

where:

A_z - the vector potential,
l_z - the stack length of the stator,
S - the surface of the cross section of the slots that carry the current of the appropriate winding,
i - the current per strand,
J - the current density.

The number of windings is considered by the dependency of the current density J from the current per strand i. One non-linear model is solved for each studied load angle. In the post-process, the appropriate distributions of J, conforming to I_d or I_q, are generated. L_d and L_q are extracted using (8). Due to the non-linear problem definition, the saturation dependencies of the inductances are found.

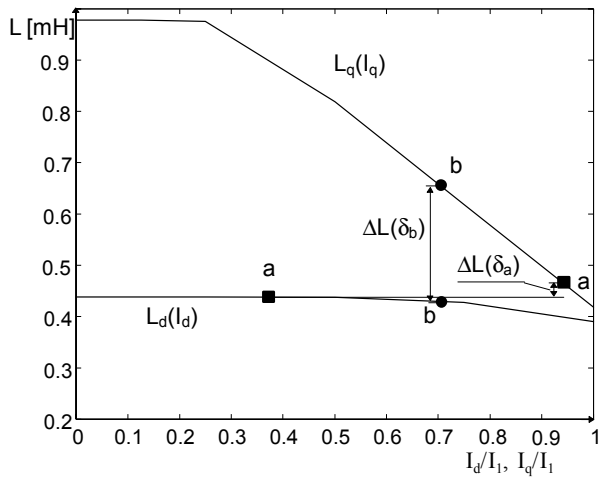

Figure 7. Inductances L_d and L_q as function of the current components I_d and I_q for two different load angles at rated current.

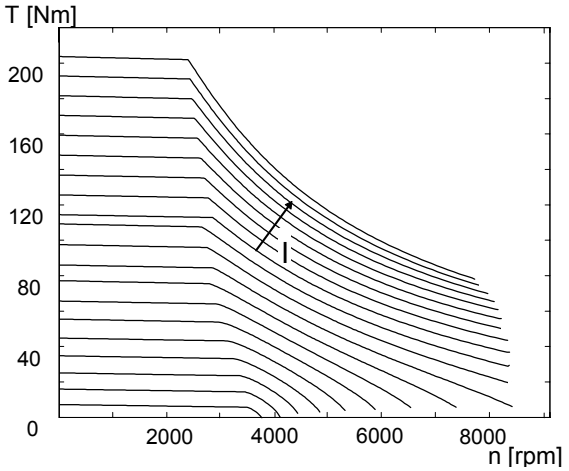

Figure 8. Torque as function of the speed obtained by static calculation of the equivalent circuit using $L_q(I,\delta)$ and $L_d(I,\delta)$.

To cover the whole operation range of the motor, the inductances L_d and L_q are computed for in the step of $\Delta\delta$=5° and ΔI=0.05*I_r. This involves 380 FE solutions. The results for I=I_r are indicated in Fig. 5. The graph shows the difference $\Delta L = L_q$-L_d for two selected load angles δ_a and δ_b. ΔL rises if δ increases, due to the saturation of the *d*-axis flux path.

This predicts the variation of the inductances $L_q(I,\delta)$ and $L_d(I,\delta)$ can be used in the control algorithm. Equation (3) becomes a differential equation $\Psi_{opt}(I,\Psi)$ and can be solved by using tables of the numerical computed values (Fig. 6,7). For real time control algorithms the inductances are approximated by polynomial functions.

THERMAL COMPUTATION

High performance for electric vehicle drives is obtained by allowing the machine to carry a load exceeding its rated values for a short period of time. The limit of such a overloading is described by the maximum temperature rise. It is essential to predict the behaviour of the machine for any time varying load. The temperature as function of the time is determined by numerical integration of the differential equations of the thermal equivalent circuit (Fig. 3). The elements of the thermal equivalent circuit can be obtained by analytical methods or the FEM and are implemented in the dynamic system of equations of the machine. The analytical calculated losses are verified by the FEM. Here, the motor model is taken from the FEM and the problem definition is provided by the analytical calculation.

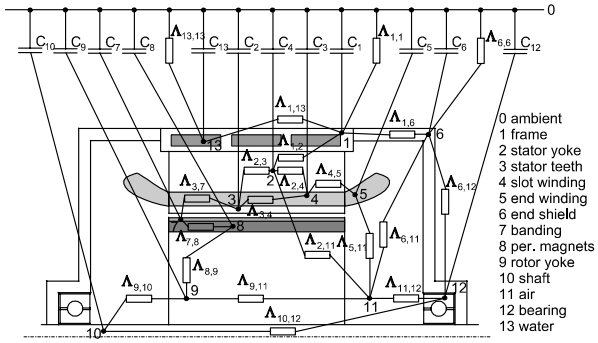

Figure 9: Thermal equivalent circuit of a water-cooled PMSM [11].

CONTROL

In an application such as an electric vehicle, invertor and motor efficiency should be as high as possible. With the rotor geometry as described earlier, advantage can be taken of the reluctance torque [e] as in the case of an interior PMSM [d], with this remark that the ratio Ld/Lq is somewhat lower for the proposed inset permanent magnet design.

The drive control algorithm has to determine at any instant the optimal torque per Ampere trajectory, regarding the additional reluctance torque [d]. This means that also in the constant torque region the id current (and thus the angle β) is varied. The required d-q currents can be calculated from the command torque, resulting in a simple feedforward torque control algorithm, as was proposed in [d]. The equations used to calculate id and iq command values rely on the motor parameters.

The torque command is normally the output of a PI controller. This output can also be considered as a stator current command and d-q components can be calculated according to (3).

Figure ?

The simple feedforward control does not take into account the operating limits of inverter driven PMSMs. In [f], the effect of the finite inverter dc bus voltage is extensively described and an additional flux-weakening feedback scheme is presented. This work was further elaborated and a modified control is proposed in [g].

Figure xx illustrates these limits in the id-iq plane. Hyperbolas of constant torque are shown, as wel as the voltage limit ellipses, the maximum current circle and the optimal torque per ampere trajectory.

Figure (torque hyperbola, voltage ellips and current circle)

The control has to cope with this varying voltage limitation, as well as current limitation and saturation

The current has to follow the torque trajectory, until the voltage limit ellips is reached. As the torque command continues along the trajectory, the maximum motor torque that can be delivered (at

constant speed) is realized by tracking the voltage limit ellips until maximum current is reached.

The voltage limit ellips becomes smaller with increasing speed, but depend also on the maximum stator voltage. Because of the presence of a varying dc bus voltage (battery voltage 240 V to 400V) in the vehicle applicaton, it is preferable to use a flux-weakening algorithm that is based on the feedback of stator-voltage command, as in [h]. For the proposed drive, this control scheme is adapted to the motor design and extended with the feedback of the measured dc bus voltage to decide on transition from constant torque to constant power region. In this way, flux-weakening starts automatically when any limit is reached and the vehicle will have maximum available performance at any dc bus voltage.

Figure? Simulation of transition into flux-weakening mode for the 45 kW motor

The inverter for the designed vehicle motor will have the ratings listed in Table xx. Its interface with the control board will be described in the next section.

EXPERIMENTAL SETUP

In order to evaluate the electric vehicle motor design and control as described above, a reduced scale prototype permanent magnet motor with surface-inset magnets was constructed and is tested in a laboratory setup. Data of this motor are shown in table 3. To check motor heating against the applied duty cycle, temperature sensors (Pt 100) are introduced only in the stator, because the rotor has no winding and serious heating of the rotor is not expected.

The inverter used is a slightly modified standard VSI-PWM inverter with IGBTs. Only an interface to galvanically isolate the control board from the inverter is added.

The motor control is implemented using a DSP based controller board [] with additional I/O features and an encoder interface. The laboratory further consists of a host PC for the controller board, the IGBT inverter, the 2.8 kW prototype motor, current sensors and an incremental encoder.

The heart of the controller board is a TMS320C31 Digital Signal Processor. A slave processor is used to perform digital input and output and generate PWM signals. The controller board can be directly programmed using MATLAB®/SIMULINK® [].

Motor currents are measured and fed to the control board by 16 bit AD converters and digitally filtered. Position is measured using an incremental encoder, of which the signals can be directly connected to the encoder interface on the controller board. This is sufficient for laboratory testing. Because of the bit selectable I/O ports on the slave processor, an absolute encoder or resolver can be used as well.

The algorithm determines reference values for direct and quadrature axis currents. The PWM generation scheme that is implemented in the slave processor is based on phase voltage reference values. For this reason, these reference values are determined using a decoupling network and the inverse Park transformations. For an electric vehicle application, the use of classical PI-controllers in the decoupling system is satisfying [5].

The dotted frame indicates the functions that are implemented on the controller board.
The current sample period has to be a multiple of the PWM period. Because the DSP can calculate the algorithm sufficiently fast, the sample rate is chosen the same as the PWM frequency, i.e. 10 kHz.

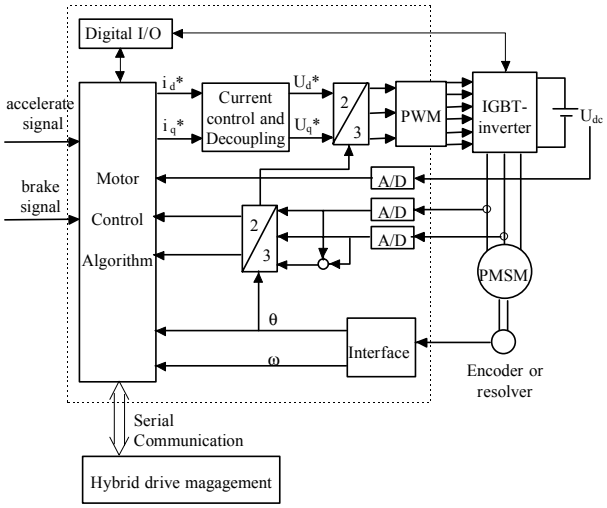

Figure 5: Control system for the PMSM.

.

Tab. 3 Data of the reduced power prototype surface-inset PMSM

ACKNOWLEDGEMENT

The authors are grateful to the Belgium Ministry of Scientific Research for granting the IUAP No. P4/20 on Coupled Problems in Electromagnetic Systems and the Council of the Belgian National Science Foundation.

REFERENCES

1. Nasar, S. A., Boldea, I., Unnewehr, L. E.: "Permanent Magnet, Reluctance, and Self-Synchronous Motors". CRC Press, 1993, London Tokyo

2. L. Chang, G. E. Dawson, T. R. Eastham; "Permanent Magnet Synchronous Motor Design: Finite Element and Analytical Methods"; ICEM Conf. Proceedings, Cambridge, pp. 1082-1088, Aug. 1990.

3. Slemon, G. R.: Xian, L.: "Modelling and Design Optimisation of Permanent Magnet Motors". Electric Machines and Power Systems, vol. 20, no. 2, pp. 71-92, April 1992.

4. Henneberger G., Hadji-Minaglou J.-R., Ciorba R. C. ; "Flux-Weakening Operations of Permanent Magnet Synchronous Motors for Electric vehicle Operation"; Workshop on Electric and Magnetic Fields, Leuven, Conf. Proceedings, pp. 57-60, May 1994.

5. Hadji-Minaglou J.-R:"Antriebskonzepte mit permanent- erregten Synchronmotoren für den einsatz im Elektrofahrzeug", PhD-thesis RWTH Aachen, jul. 1994.

6. Nipp, E.: "Alternative to Field Weakening of Surface Mounted Permanent Magnet Motors for Variable Speed Drives". Proc. IAS'95, pp. 191-198.

[5] G. Henneberger, S. Domack and J. Berndt, "Comparison of the Utilization of Brushless DC Servomotors with Different Rotor Length y 3D - Finite Element Analysis", *IEEE Transactions on Magnetics*, vol. 30, no. 5, pp. 3675-3678, 1994

[6] D. Taghezout and P. Lombard, "Finite Element Prediction of a Brushless DC Motor Dynamical Behaviour", *2nd EPE Chapter Symposium on Electric Drive Design and Applications*, Nancy, France, June 4-6, 1996, Conf. Proc. pp. 47-52

Fig. 3: Torque as function of the motor speed

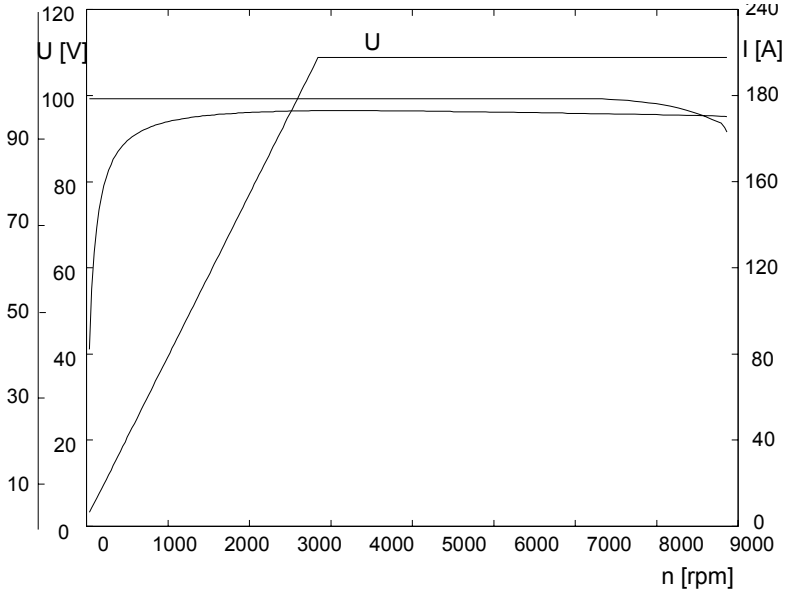

Fig. 4: Terminal voltage, stator current at maximum torque and efficiency as function of the motor speed

[a] Rotor-position-controlled permanent magnet synchronous machines for electrical vehicles
K.J Binns, B. Sneyers, G. Maggetto, Ph. Lataire
Proceeding of the International Conference on Electrical Machines, September 1980, Athens, pp. 346-357

[b] Inverter fed permanent magnet synchronous motor road electric traction
B. Sneyers, G. Maggetto, J.L. Van Eck
Proceeding of the International Conference on Electrical Machines, September 1982, Budapest, pp. 550-553

[c] Field weakening in buried permanent magnet AC motor drives
B.Sneyers, D.W.Novotny,T.A.Lipo
IEEE Transactions on Industry Applications, Vol. IA-21,No.2, March/April 1985

[d] Interior permanent magnet synchronous motors for adustable -speed drives
T.M. Jahns, G.B. Kliman, T.W. Neumann
IEEE Transactions on Industry Applications, Vol. IA-22,No.4, July/August 1986

[e] Operating limits of inverter-driven permanent magnet motor drives
T. Sebastian, G.R.Slemon
IEEE Transactions on Industry Applications, Vol. IA-23,No.2, March/April 1987

[f] Flux-weakening regime operation of an interior permanent-magnet synchronous motor drive
T.M. Jahns
IEEE Transactions on Industry Applications, Vol. IA-23, No.4, July/August 1987

[g] Control techniques for improved high-speed performance of interior PM synchronous motor drives
Stephen R. Macminn, Thomas M. Jahns
IEEE Transactions on industry applications, Vol 27, nr. 5 September/October1991, pp.997-1004

[h]. Kim, J.-M. Sul S.-K.: "Speed Control of Permanent Magnet Synchronous Motor Drive for Flux Weakening Operations". Proc. IAS'95, pp. 216-221.

[i]. Zhong L., Rahman M.F., Lim K.W.; Modelling and experimental studies of an instantaneous torque and field weakening control scheme for an interior permanent magnet synchronous motor drive**,** Proceedings of ELECTRIMACS 1996, pp. 297-302.